JCB Article

Targeting of U4/U6 small nuclear RNP assembly factor SART3/p110 to Cajal bodies

David Staněk,[1] Stephen D. Rader,[2] Mirko Klingauf,[1] and Karla M. Neugebauer[1]

[1]Max Planck Institute of Molecular Cell Biology and Genetics, 01307 Dresden, Germany
[2]Department of Biochemistry and Biophysics, University of California, San Francisco, CA, 94143

The spliceosomal small nuclear RNAs (snRNAs) are distributed throughout the nucleoplasm and concentrated in nuclear inclusions termed Cajal bodies (CBs). A role for CBs in the metabolism of snRNPs has been proposed but is not well understood. The SART3/p110 protein interacts transiently with the U6 and U4/U6 snRNPs and promotes the reassembly of U4/U6 snRNPs after splicing in vitro. Here we report that SART3/p110 is enriched in CBs but not in gems or residual CBs lacking coilin. The U6 snRNP Sm-like (LSm) proteins, also involved in U4/U6 snRNP assembly, were localized to CBs as well. The levels of SART3/p110 and LSm proteins in CBs were reduced upon treatment with the transcription inhibitor α-amanitin, suggesting that CB localization reflects active processes dependent on transcription/splicing. The NH_2-terminal HAT domain of SART3/p110 was necessary and sufficient for specific protein targeting to CBs. Overexpression of truncation mutants containing the HAT domain had dominant negative effects on U6 snRNP localization to CBs, indicating that endogenous SART3/p110 plays a role in targeting the U6 snRNP to CBs. We propose that U4 and U6 snRNPs accumulate in CBs for the purpose of assembly into U4/U6 snRNPs by SART3/p110.

Introduction

The cell nucleus contains numerous, morphologically distinct domains and bodies. One of these, a 0.5–1.0-μm sphere named the Cajal body (CB),* was discovered 100 yr ago by Santiago Ramón y Cajal. The molecular characterization of CBs has been facilitated by the discovery of the protein coilin, an unambiguous marker of CBs in *Xenopus*, mouse, and human cells (Raska et al., 1990, 1991; Andrade et al., 1991; Tuma et al., 1993). Coilin likely plays an important role in cell metabolism because coilin knockout mice exhibit reduced viability (Tucker et al., 2001). Many factors involved in transcription, RNA processing, and cell cycle regulation are concentrated in CBs, but the function of CBs, with respect to these diverse processes, remains obscure (Matera, 1999; Gall, 2000). Although spliceosomal U1, U2, U4, U5, and U6 small nuclear RNAs (snRNAs) are enriched in CBs (Carmo-Fonseca et al., 1991, 1992; Matera and Ward, 1993), CBs are not likely sites of splicing because they are not transcriptionally active and lack many essential non-snRNP splicing factors (Matera, 1999; Raska et al., 1991). snRNP association with CBs is transcription dependent, indicating that CBs play an active role in snRNP metabolism and may be the sites of snRNP assembly rather than storage of inactive snRNPs (Carmo-Fonseca et al., 1992; Ogg and Lamond, 2002). What essential function accounts for the concentration of spliceosomal snRNPs in CBs?

The U1, U2, U4, and U5 snRNAs are synthesized by RNA polymerase II, capped at their 5′ ends, and transported to the cytoplasm where they are bound by snRNP-specific Sm proteins (for reviews see Will and Luhrmann, 2001; Paushkin et al., 2002). These snRNAs are hypermethylated at their 5′ ends, producing their characteristic 2,2,7 trimethylguanosine (TMG) caps and providing an important signal for snRNP import into the nucleus (Hamm et al., 1990). Because snRNP-specific proteins appear to concentrate in CBs before accumulating in the nucleoplasm, a role for CBs in the maturation of snRNPs has been proposed (Sleeman and Lamond, 1999; Sleeman et al., 2001; Ogg and Lamond, 2002). The recent identification of RNAs that guide base modification of snRNAs and localization of these guide RNAs to CBs suggest that snRNA base modification may take place in CBs (Carmo-Fonseca, 2002; Darzacq et al., 2002; Kiss, 2002; Kiss et al., 2002). However, these results

Address correspondence to Karla Neugebauer, Ph.D., Max Planck Institute of Molecular Cell Biology and Genetics, Pfotenhauerstrasse 108, 01307 Dresden, Germany. Tel.: 49-351-2102589. Fax: 49-351-2101209.
E-mail: neugebauer@mpi-cbg.de

*Abbreviations used in this paper: CB, Cajal body; LSm, like Sm; RRM, RNA recognition motif; SFC, splicing factor compartment; SMN, survival of motor neuron protein; sn, small nuclear; TMG, 2,2,7-trimethylguanosine.

Key words: RNA splicing; coiled (Cajal) body; U4/U6 small nuclear ribonucleoprotein; small nuclear RNA; nuclear proteins

do not explain why the U6 snRNA, which is synthesized by RNA polymerase III, is not capped or exported to the cytoplasm, and undergoes base modification in the nucleolus (Tycowski et al., 1998; Ganot et al., 1999; Lange and Gerbi, 2000), is present in CBs. The U6 snRNA is present in at least three distinct snRNPs, the U6 snRNP, the U4/U6 snRNP, and the U4/U6•U5 tri-snRNP. Formation of all of these snRNP species must occur in the nucleus, but little is known about the subnuclear location of these processes.

After assembly, the U1, U2, and U4/U6•U5 snRNPs perform essential functions in spliceosome formation and catalysis. During a process termed the spliceosomal cycle, each snRNP is thought to participate in subsequent rounds of splicing, which then requires the regeneration of snRNPs that have undergone rearrangement during splicing (Staley and Guthrie, 1998). In particular, the U4/U6 snRNP, which contains two snRNAs base paired with each other, unwinds during splicing as U6 establishes new base-pairing interactions with U2 and the pre-mRNA. Therefore, U4 and U6 must reanneal after splicing to regenerate functional U4/U6 snRNPs. In yeast, the essential protein Prp24 catalyzes this reaction (Raghunathan and Guthrie, 1998; Rader and Guthrie, 2002). In the absence of Prp24p, splicing extracts are depleted of the U4/U6 snRNP, demonstrating the importance of snRNP recycling for continuing rounds of pre-mRNA splicing (Raghunathan and Guthrie, 1998).

Recently, the tumor rejection antigen SART3/p110 was identified as the human homologue of Prp24p (Bell et al., 2002; Rader and Guthrie, 2002) and was shown to be required for U4/U6 snRNP recycling in vitro (Bell et al., 2002). SART3/p110 binds specifically and directly to the U6 snRNA and is detectable in the U6 and U4/U6 snRNPs (Bell et al., 2002). Unlike other U4, U5, and U6 snRNP–specific proteins, SART3/p110 is not detectable in the U4/U6•U5 tri-snRNP (Bell et al., 2002; Schneider et al., 2002), indicating that SART3/p110 dissociates from its U4 and U6 snRNP substrates once they are annealed. In addition to SART3/p110, the Sm-like (LSm) proteins LSm2–8, which assemble on the 3′ end of the U6 snRNA as a stable heteromer and persist in the U4/U6 and U4/U6•U5 snRNPs (Seraphin, 1995; Gottschalk et al., 1999; Salgado-Garrido et al., 1999; Vidal et al., 1999; Schneider et al., 2002), have been implicated in U4/U6 snRNP assembly (Achsel et al., 1999; Mayes et al., 1999). The LSm proteins bind directly to Prp24 in yeast (Fromont-Racine et al., 2000; Rader and Guthrie, 2002; Ryan et al., 2002), providing a second mode of interaction with the U6 snRNP. In vitro, Prp24p anneals U4 and U6 snRNAs more efficiently in the context of snRNPs (Raghunathan and Guthrie, 1998), making it likely that the combination of SART3/p110/Prp24p and LSm proteins enables efficient assembly of the U4/U6 snRNP in vivo. Because the role of SART3/p110 in U4/U6 recycling is uniquely transient, the subnuclear distribution of SART3/p110 has the potential to reveal the sites of U4/U6 snRNP assembly.

In this study, we report that SART3/p110 and the LSm proteins, LSm4 and LSm8, are localized in the cell nucleus and concentrated in CBs. We studied the association of SART3/p110 and snRNPs with CBs after transcription inhibition and run-on treatment and in the absence of the CB component coilin. SnRNP and SART3/p110 localizations in CBs were correlated in each of these experimental conditions. Mutant analysis revealed that the HAT domain of SART3/p110 represents the major determinant for specific targeting of SART3/p110 to CBs. Overexpression of mutants lacking the snRNP-binding COOH-terminal domains reduced the concentration of both endogenous SART3/p110 and LSm4 in CBs, suggesting that SART3/p110 is required for U6 snRNP targeting to CBs.

Results

By immunofluorescent labeling of HeLa cells, SART3/p110 was detected exclusively in the cell nucleus, where it was distributed throughout the nucleoplasm and specifically enriched in large bright dots (Fig. 1, A and B). Double labeling of cells for SART3/p110 and the TMG cap (Fig. 1 A), a modification found at the 5′ end of U1, U2, U4, and U5 snRNAs, revealed complete overlap between SART3/p110

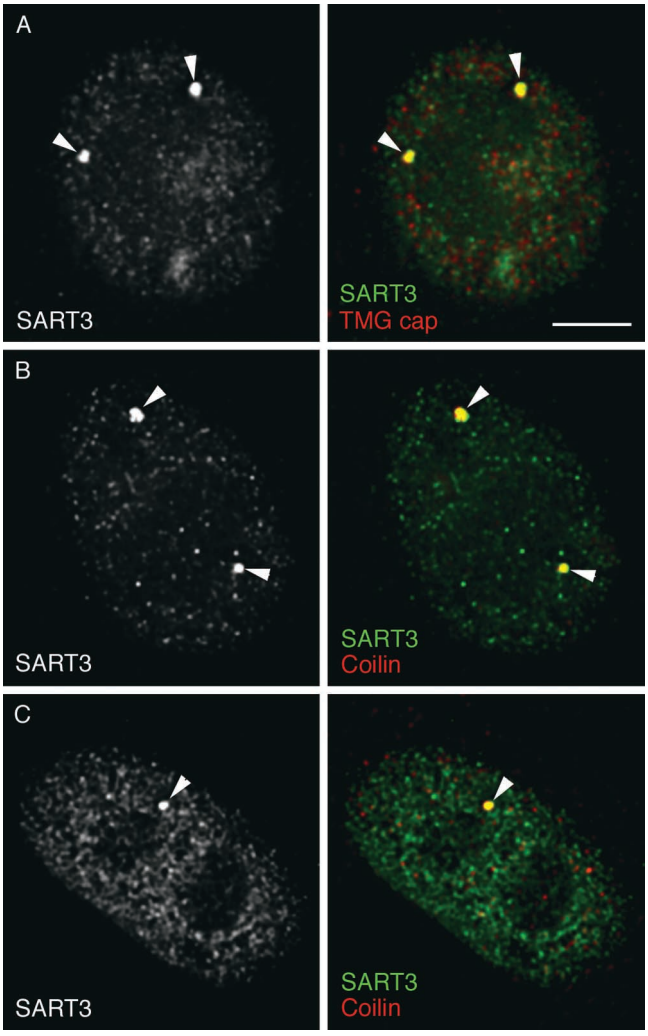

Figure 1. **SART3/p110 is concentrated in CBs.** (A and B) Immunolocalization of SART3/p110 in HeLa cells together with (A) TMG cap, a marker of snRNPs, or (B) with coilin, a marker of CBs. (C) SART3/p110 and coilin were immunolocalized in human primary fibroblasts WI-38. CBs are marked by arrowheads. Bar, 5 μm.

and snRNPs in the large bright structures. These bodies were identified as CBs by double detection of SART3/p110 and coilin, a marker of CBs (Fig. 1 B). SART3 was detected in all observed CBs ($n = 51$ cells). The same results were obtained in cells transiently expressing SART3/p110 conjugated to EGFP (see below and Fig. 7). Measurement of endogenous SART3/p110 fluorescent intensities in CBs revealed that the concentration of SART3/p110 in CBs is approximately three times higher then in the nucleoplasm (see below, Table I). We confirmed the SART3/p110 localization patterns in WI-38 primary human fibroblasts (Fig. 1 C). Although the fibroblasts contain fewer CBs, SART3/p110 was concentrated in every CB observed. In contrast to the striking overlap between SART3/p110 and snRNPs in CBs, only partial colocalization of SART3/p110 and snRNPs was observed in the nucleoplasm (Fig. 1 A).

The survival of motor neuron protein (SMN) is involved in the assembly of snRNPs in the cytoplasm (Fischer et al., 1997; Massenet et al., 2002). In addition, SMN and associated gemin proteins are detected in the cell nucleus in structures termed gems (Liu and Dreyfuss, 1996). Gems often overlap or are associated with CBs, depending on the cell type (Carvalho et al., 1999; Young et al., 2000). The function of nuclear SMN is currently unknown, although roles in splicing and transcription have been hypothesized (Pellizzoni et al., 1998, 2001). Because a role for gems in snRNP recycling has been proposed, we tested whether SART3/p110 specifically localizes to gems in a HeLa cell line in which gems are often separate from CBs. Double staining of HeLa cells with anti-SART3/p110 and anti-SMN antibodies (Fig. 2 A) revealed that SART3/CBs were overlapping or adjacent to gems only 58% of the time ($n = 55$ cells). Like the HeLa cell line, WI-38 primary fibroblasts often contained gems independent from CBs. We did not detect any enrichment of SART3/p110 in gems in primary fibroblasts (Fig. 2 B). Because 100% of CBs contain SART3/p110 (see above), we conclude from this result that gems, per se, are not sites of SART3/p110 accumulation.

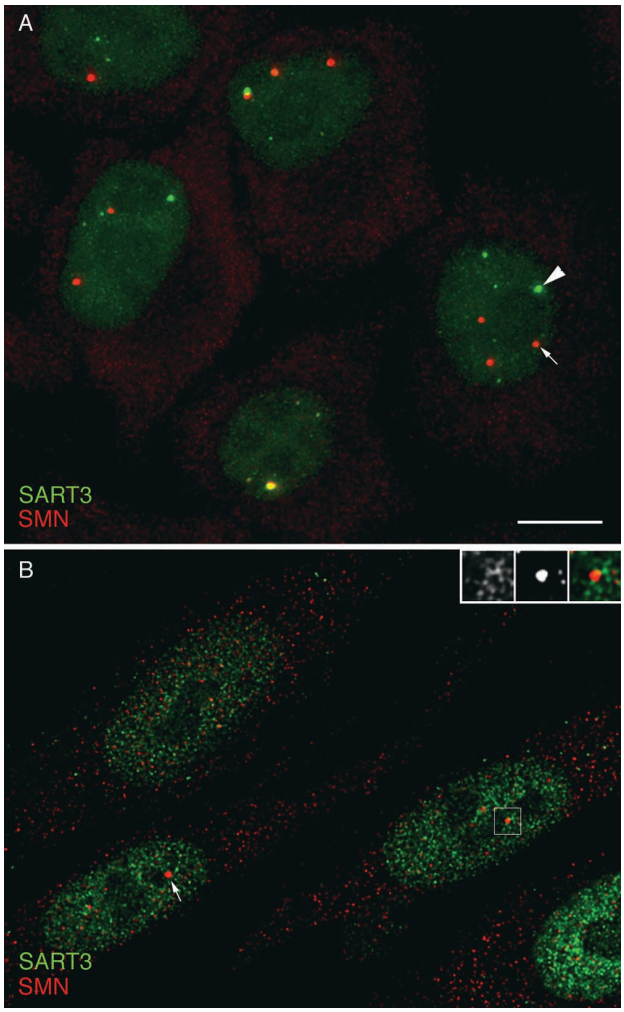

Figure 2. **SART3/p110 is not specifically localized in gems.** SART3/p110 and SMN, enriched in gems, were immunolocalized in (A) HeLa cells and (B) human primary fibroblasts WI-38. Examples of CBs are marked by arrowheads, gems by arrows. Inserts are magnified two times, and green (left), red (middle), and merged (right) signals are shown. Bar, 10 μm.

To investigate the targeting of SART3/p110 to CBs, we analyzed the role of coilin in SART3/p110 recruitment to CBs. We compared the distribution of SART3/p110 in embryonic fibroblasts derived from a wild-type mouse versus a mouse in which both coilin alleles were disrupted (Tucker et al., 2001). Wild-type mouse embryonic fibroblasts have snRNPs, SMN, fibrillarin, and Nopp140 localized in CBs (Tucker et al., 2001; Fig. 3). In embryonic fibroblasts derived from the coilin knockout mouse, fibrillarin and Nopp140 are accumulated in so-called "residual" CBs, which fail to recruit snRNPs and SMN; snRNPs are distributed throughout the nucleoplasm, and SMN is concentrated in separate gems (Tucker et al., 2001). Similar to our previous results, we found that SART3/p110 was detected in the nucleoplasm and in CBs of coilin$^{+/+}$ cells, labeled either by anti–TMG cap, anti-fibrillarin, or anti-SMN antibodies (Fig. 3, A, C, and E). In coilin$^{-/-}$ cells, SART3/p110 was distributed throughout the nucleoplasm with no detectable concentration in residual CBs (Fig. 3 B) or gems (Fig. 3 D). Double staining of coilin$^{-/-}$ cells with anti–TMG cap and SART3/p110 antibodies revealed the distribution of snRNPs and SART3/p110 throughout the nucleoplasm and never in the highly concentrated sites detectable in wild-type cells (Fig. 3, compare E with F). Thus, coilin expression is required for the recruitment of both snRNPs and SART3/p110 to CBs.

Splicing largely occurs at transcription sites (for review see Neugebauer, 2002). To test the possibility that SART3/p110 is cotranscriptionally recruited to snRNPs, we labeled nascent RNA with BrUTP and visualized labeled RNA together with SART3/p110 (Fig. 4 A). Nucleoplasmic SART3/p110 did not appreciably overlap with transcription sites. During the course of these experiments, we noticed that cells permeabilized under run-on conditions (see Material and methods) exhibited a dramatic loss of SART3/p110 from CBs (compare Fig. 4 B with Fig. 1 B). We have further investigated this phenomenon and found that snRNPs were also largely extracted from CBs during run-on transcription as revealed by TMG cap labeling (Fig. 4 C). In contrast, run-on treatment did not affect the detection of coilin, fibrillarin, or SMN in CBs and/or gems (Fig. 4 C). This sug-

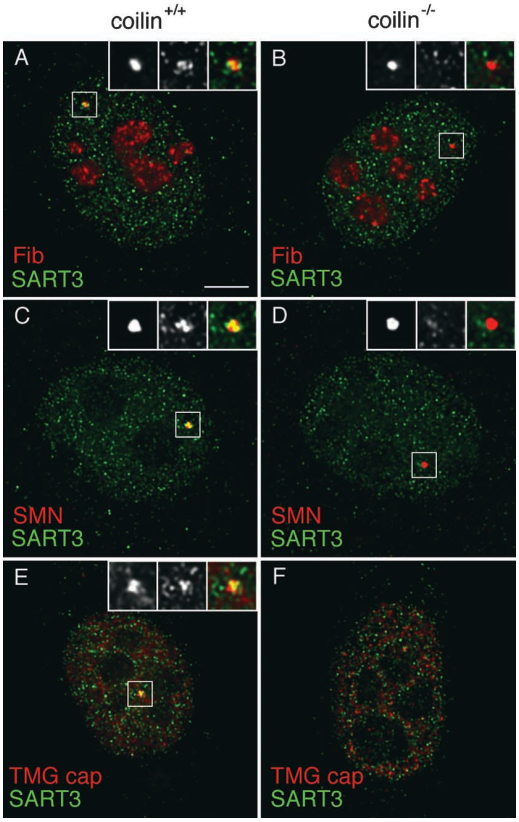

Figure 3. **SART3/p110 recruitment to CBs requires coilin.** Mouse embryonic fibroblasts derived from control (coilin$^{+/+}$) or coilin knockout (coilin$^{-/-}$) mice were stained for SART3/p110 together with (A and B) fibrillarin (Fib), (C and D) SMN, and (E and F) TMG cap. (A, C, and E) In control coilin$^{+/+}$ cells, SART3/p110 concentrates in CBs labeled by fibrillarin, SMN, and TMG cap (Tucker et al., 2001). (B, D, and F) In cells lacking functional coilin, SART3/p110 is distributed throughout the nucleoplasm and is not recruited to residual CBs labeled by fibrillarin (B) or gems labeled by SMN (D). No CBs were detected by TMG cap (F). Inserts are magnified two times, and red (left), green (middle), and merged (right) signals are shown. Bar, 5 μm.

gests that snRNPs and SART3/p110 are only weakly associated with CBs, compared with the apparently more stable components, coilin, SMN, and fibrillarin.

The presence of U4 and U6 snRNAs (Carmo-Fonseca et al., 1992; Matera and Ward, 1993) and SART3/p110 in CBs indicates that CBs contain the substrates and at least one factor required for U4/U6 snRNP assembly. To determine whether the U6 snRNA–associated LSm proteins that promote U4/U6 annealing in vitro (Achsel et al., 1999) are also present in CBs, we analyzed the distribution of two members of the LSm complex. By immunofluorescence, LSm4 was detected both in the cytoplasm and the nucleus (Fig. 5, A and B). The cytoplasmic localization may represent LSm complexes involved in mRNA degradation (Bouveret et al., 2000; Tharun et al., 2000). In the nucleus, LSm4 was detected throughout the nucleoplasm and concentrated in CBs (Fig. 5 A). Double staining of HeLa cells with anti-LSm4 and anti–TMG cap antibodies revealed complete overlap of both antigens in CBs but only partial overlap in the nucleoplasm (Fig. 5 B). Similarly, LSm8 tagged with EYFP was mainly detected in the nucleoplasm and in CBs (Fig. 5 C) where it colocalized with LSm4 (Fig. 5 D). Although LSm proteins participate in several distinct complexes, including the *Xenopus laevis* U8 small nucleolar RNP (Tomasevic and Peculis, 2002) and a cytoplasmic mRNA degradation complex (Bouveret et al., 2000; Tharun et al., 2000), it is likely that localization of LSm4 and LSm8 reflects the presence of the mature U6 snRNP in CBs.

The observations that SART3/p110, snRNPs, and LSm proteins are concentrated in CBs (Figs. 1 and 5) and that snRNP and SART3/p110 association with CBs is correlated (Figs. 3 and 4) combine to suggest that SART3/p110 may accumulate in CBs for the purpose of U4/U6 snRNP assembly. However, an alternative hypothesis is that SART3/p110 is inactive and perhaps stored in CBs. To distinguish between these possibilities, we tested whether SART3/p110 concentration in CBs was affected by transcription activity in the cell. It was previously shown that depleting the cell of pre-mRNA by blocking RNA polymerase II activity leads to a reduction in overall snRNP concentration in CBs (Carmo-Fonseca et al., 1992). If SART3/p110 is stored in the CB, one would expect SART3/p110 levels to remain constant or even increase upon transcription inhibition. If, in contrast, SART3/p110 in CBs is active in U4/U6 snRNP assembly, then SART3/p110 levels in CBs should decrease when transcription is inhibited.

To determine whether SART3/p110 concentration in CBs is dependent on RNA synthesis, cells were treated with the transcription inhibitor α-amanitin. After treatment, all cells had rounded splicing factor compartments (SFCs) labeled with SC-35 (Fig. 6, A and B), an indication of RNA polymerase II inhibition (Carmo-Fonseca et al., 1992). Neither SART3/p110 nor LSm4 was enriched in SFCs. The latter result was unexpected, because other snRNPs (U1, U2, U4, and U5) have been shown to concentrate in SFCs after α-amanitin treatment (Carmo-Fonseca et al., 1992; Blencowe et al., 1993). After α-amanitin treatment, two types of coilin-positive CBs were observed: normal-looking CBs (indistinguishable from CBs in nontreated cells in size and morphology) and enlarged "ring-shaped" CBs, as reported previously (Carmo-Fonseca et al., 1992; Haaf and Ward, 1996; Frey et al., 1999). This change in CB morphology is not likely to reflect cell death because ~95% of the cells were viable, according to a standard viability test (see Material and methods). In contrast to control untreated cells (Figs. 1 and 5), we did not detect any specific enrichment of SART3/p110 or LSm4 in any of the coilin-labeled CBs (Fig. 6, C and D). Quantitation of the fluorescence intensities within normal-looking CBs relative to the nucleoplasmic signal revealed that SART3/p110 levels in CBs decreased threefold ($P < 0.0001$) and LSm4 levels in CBs decreased twofold ($P < 0.0001$) after α-amanitin treatment. These results indicate that SART3/p110 and LSm4 association with CBs is transcription/splicing dependent and not likely due to the storage of inactive molecules.

To determine how SART3/p110 is specifically localized to CBs, we investigated the potential of isolated SART3/p110 protein domains fused with EGFP to target CBs. Human SART3/p110 is composed of three major protein domains, a repeat of seven HAT (half a TPR domain) motifs followed by a nuclear localization signal, two RNA recogni-

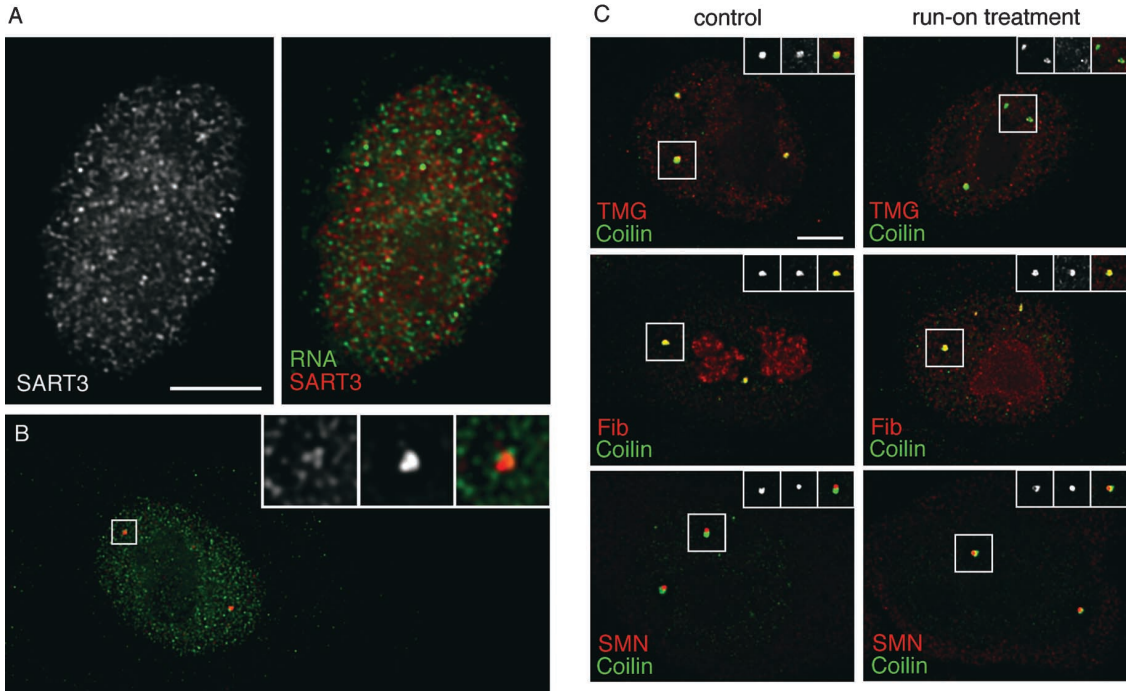

Figure 4. **SART3/p110 is depleted from CBs after nuclear run-on.** (A) Cells were permeabilized using run-on conditions (see Materials and methods), and newly synthesized RNA was labeled by BrUTP and detected together with SART3/p110. Little colocalization of SART3/p110 with labeled RNA was detected. (B) Cells after run-on treatment were labeled for SART3/p110 and coilin. (B, inset) Representative CB was magnified 3.5 times, and green (left), red (middle), and merged (right) signals are shown. (C) Control fixed cells (control) and cells after run-on (run-on) labeled with coilin together with TMG cap, fibrillarin (Fib), and SMN. For representative CBs, green (left), red (middle), and merged (right) signals are shown in the insets. Bars: (A and C) 5 μm; (B) 10 μm.

tion motifs (RRMs), and the highly conserved COOH-terminal domain CT10 (Fig. 7 A; Bell et al., 2002; Rader and Guthrie, 2002). The HAT domains and their related TPR domains are present in a number of other RNA processing factors and have been hypothesized to function in protein–protein interactions (Preker and Keller, 1998; Zhou et al., 2002). Recently, the SART3/p110 HAT domain was shown to interact with the HIV-1 Tat protein (Liu et al., 2002). The RRMs have been implicated in U6 snRNA binding (Shannon and Guthrie, 1991; Bell et al., 2002), and the CT10 domain likely mediates binding to the U6 snRNP via interaction with LSm proteins, as it does in yeast (Rader and Guthrie, 2002). In two-hybrid assays, full-length SART3/p110 interacted specifically with LSm7 but not with LSm1, which is not present in the U6 snRNP. Deletion of the CT10 domain reduced the two-hybrid interaction twofold, suggesting that the CT10 domain contributes to SART3/p110 binding to the U6 snRNP via LSm proteins (unpublished data). We created several EGFP-tagged proteins composed of specific SART3/p110 domains (Fig. 7 A). Note that each fusion protein diagrammed (except N-TERM) was also produced with the EGFP tag at the NH_2 terminus, and the results were identical to those obtained with the COOH-terminal–tagged constructs (unpublished data), indicating that the protein localization results described below are not due to the addition of the tags at the COOH termini.

The full-length SART3/p110–EGFP (WT) revealed the same distribution as endogenous SART3/p110 (Fig. 7 B, WT; compare with Fig. 1); it localized to the nucleoplasm and was concentrated in CBs, as judged by coilin staining. Deletion of the highly conserved COOH-terminal domain CT-10 (ΔCT10) or both CT-10 and the two RNA recognition motifs (ΔCT10ΔRRM) resulted in similar localization patterns as full-length SART3/p110. In contrast, truncation of the NH_2-terminal portion of the protein containing seven HAT repeats (ΔHAT) had strong effects on protein localization. The ΔHAT–EGFP protein was found in the nucleoplasm and concentrated in nucleoli, but was only weakly detectable in CBs. Because EGFP conjugated to an NLS (EGFP–NLS) was also concentrated in nucleoli and faintly detectable in CBs, the simplest interpretation of the data is that the concentration of ΔHAT–EGFP in nucleoli and weak detectability in CBs is nonspecific. To further investigate the role of the NH_2 terminus, we created a mutant containing only the HAT domain and the endogenous NLS (HAT). This construct was specifically targeted to CBs. In contrast, the extreme NH_2-terminal region of SART3/p110 (N-TERM), lacking the HAT domain and conjugated to EGFP plus a heterologous NLS, was not specifically local-

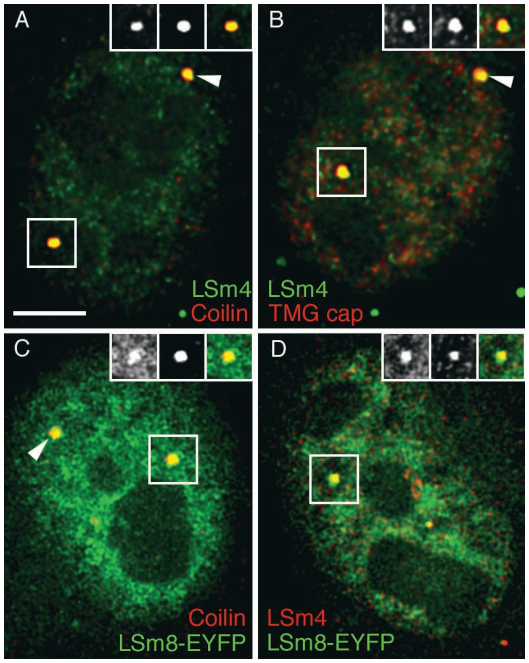

Figure 5. **U6 snRNP proteins LSm4 and LSm8 are enriched in CBs.** HeLa cells stained for LSm4 and (A) coilin or (B) TMG cap. LSm4 is concentrated in CBs, where it colocalizes with TMG cap, whereas there is only partial overlap of LSm4 with TMG cap in the nucleoplasm. HeLa cells expressing LSm8–EYFP stained for (C) coilin or (D) Lsm4. LSm8 is diffusely distributed in the cell nucleus and concentrated in CBs. Examples of CBs are marked by arrowheads. For representative CBs, green (left), red (middle), and merged (right) signals are shown in the insets. Bar, 5 μm.

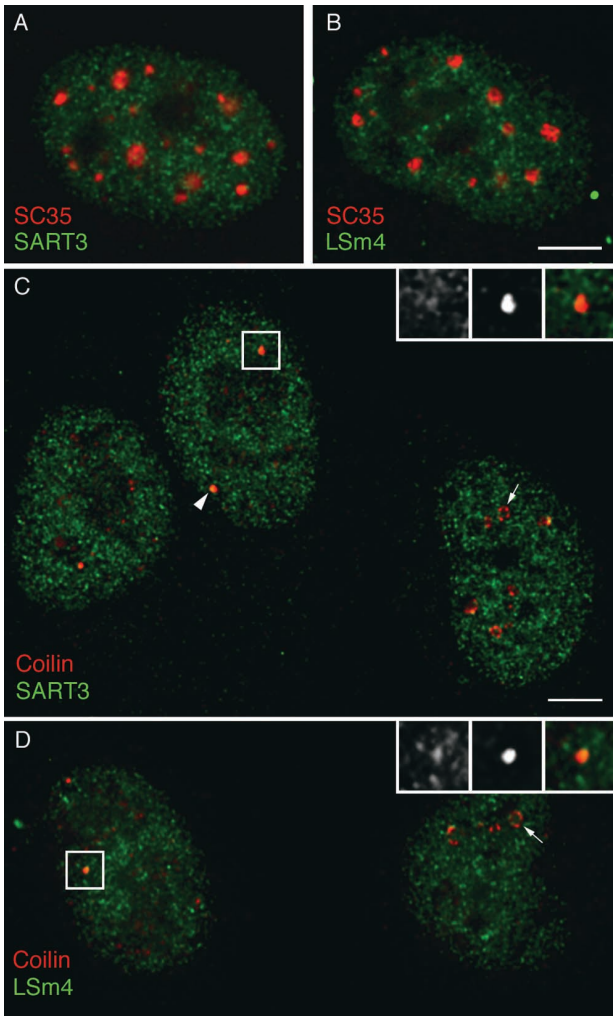

Figure 6. **SART3/p110 and LSm4 are depleted from CBs after transcription inhibition.** (A and B) HeLa cells were treated with α-amanitin and stained for a marker of splicing factor compartments (SC-35) and (A) SART3/p110 or (B) LSm4. Enlarged, rounded-up splicing factor compartments indicate that inhibition of RNA polymerase II transcription was effective. (C and D) HeLa cells after α-amanitin treatment stained with anti-coilin antibody together with (C) anti-SART3/p110 or (D) anti-LSm4 antibodies. Two types of coilin-labeled structures were observed: normal-looking CBs (arrowheads) and enlarged ring-shaped CBs (arrows). Depicted areas containing CBs were enlarged two times (insets), and green (left), red (middle), and merged (right) signals are shown. Bars, 5 μm.

ized to CBs (compare N-TERM with EGFP–NLS localizations). Interestingly, the N-TERM mutant was not highly concentrated in nucleoli, in contrast to EGFP–NLS alone. Although the function of the extreme NH_2-terminal region of SART3/p110 is currently unknown, these results suggest that it may interact with a nucleoplasmic component. We conclude from this analysis that the HAT domain of SART3/p110 is necessary and sufficient for the specific targeting of SART3/p110 to CBs.

The highly conserved CT10 domain was previously shown to interact with LSm proteins (Rader and Guthrie, 2002). To determine whether overexpression of SART3/p110 mutants lacking the COOH-terminal region affects the localization of endogenous SART3/p110 and/or LSm4, we transfected HeLa cells with WT–, ΔHAT–, ΔCT10–, and ΔCT10ΔRRM–EGFP mutants and determined the localization patterns of endogenous SART3/p110 and LSm4 by immunofluorescence (Fig. 8, WT–EGFP and ΔCT10ΔRRM–EGFP constructs shown only). Quantitation of fluorescence intensities within CBs relative to the nucleoplasm revealed that the localization of endogenous SART3/p110 was significantly reduced in ΔCT10- and ΔCT10ΔRRM-expressing cells, compared with untransfected controls (Table I). This indicates that both mutant proteins effectively compete for SART3/p110 binding sites within CBs. Moreover, if SART3/p110 plays a role in U6 snRNP localization to CBs, then expression of ΔCT10 and/or ΔCT10ΔRRM mutants may have dominant negative effects on LSm4 localization in CBs. Indeed, LSm4 concentration in CBs was significantly reduced upon overexpression of ΔCT10 or ΔCT10ΔRRM mutants by ∼30% (Table I). The expression of WT–EGFP also influenced the concentration of LSm4 in CBs, but the effect was less pronounced than in the case of ΔCT10 or ΔCT10ΔRRM mutant (Table I). We noticed that CBs were disrupted in some cells expressing high levels of ΔCT10 or ΔCT10ΔRRM mutant (unpublished data). The ΔHAT–EGFP mutant, which is aberrantly localized to nucleoli, did not show any effects on a localization of LSm4 (unpublished data). These data suggest that SART3/p110 plays a role in U6 snRNP targeting to CBs, largely through the CT10 domain of SART3/p110.

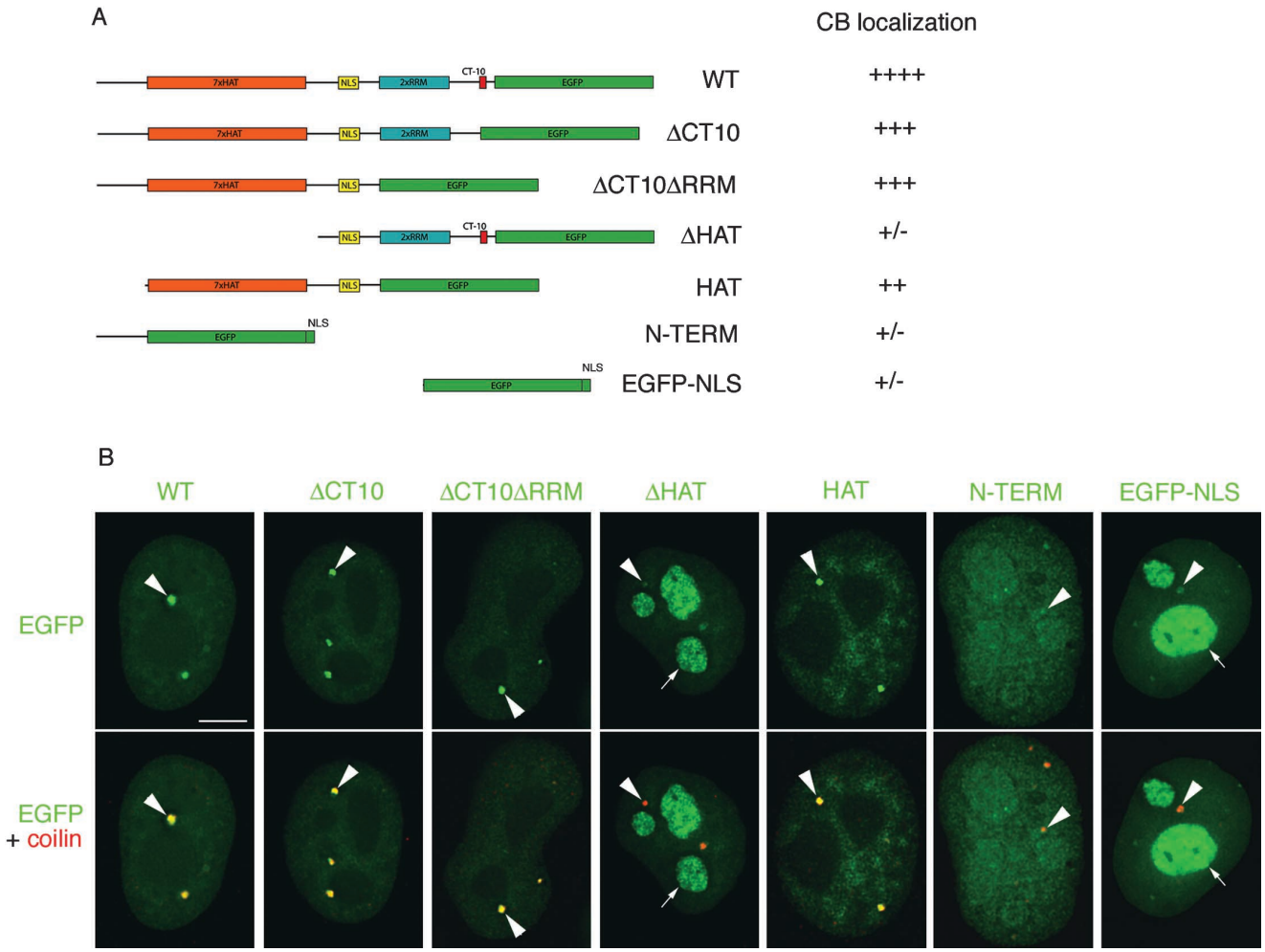

Figure 7. **The NH_2-terminal domain containing the HAT motifs targets SART3/p110 to CBs.** (A) Wild-type (WT) SART3/p110 was conjugated to EGFP. Deletion mutants containing amino acids 1–950 (ΔCT10), 1–702 (ΔCT10ΔRRM), 581–963 (ΔHAT), and 119–702 (HAT) were conjugated to EGFP. The expression construct (N-TERM) encodes the NH_2-terminal amino acids 1–127 fused to EGFP and a heterologous NLS signal. (B) All constructs including empty vector containing heterologous NLS (EGFP–NLS) were transiently expressed in HeLa cells and stained for coilin. Full-length protein as well as mutants containing the HAT domain accumulated in CBs (arrowheads). The ΔHAT protein and EGFP–NLS accumulated in nucleoli (arrows) and only weakly in CBs. The N-TERM mutant was detected throughout the nucleoplasm and slightly accumulated in nucleoli and CBs. The identification of nucleoli was verified by phase contrast microscopy (not depicted). Bar, 5 μm.

Discussion

SART3/p110 is concentrated in CBs

The CB is a nuclear structure identified in many organisms and cell lines, but little is known about its formation and function (Matera, 1999; Gall, 2000; Ogg and Lamond, 2002). In this study, we show for the first time that SART3/p110, a protein transiently associated with U4/U6 snRNP and with a defined function in the U4/U6 snRNP assembly (Bell et al., 2002), is concentrated in CBs. In HeLa cells, primary human fibroblasts, and mouse embryonic fibroblasts, we detected SART3/p110 by immunofluorescence throughout the nucleoplasm and enriched in CBs, where snRNPs were also highly concentrated. The localization of SART3/p110 in CBs was confirmed by expression of EGFP-tagged SART3/p110. Previous studies demonstrated the nuclear localization of SART3/p110 (Gu et al., 1998; Harada et al., 2001; Liu et al., 2002), but these experiments did not specifically address whether SART3/p110 was detectable in CBs. We did not find any significant overlap of nucleoplasmic SART3/p110 with sites of RNA synthesis, consistent with SART3/p110's absence from the U4/U6•U5 tri-snRNP and spliceosomes (Bell et al., 2002; Rappsilber et al., 2002; Zhou et al., 2002) and further suggesting that SART3/p110 is not recruited to snRNPs cotranscriptionally.

To address how SART3/p110 is specifically targeted to CBs, we constructed and expressed EGFP fusion proteins containing distinct domains of SART3/p110. We found that the SART3/p110 HAT domain with NLS is necessary and sufficient to specifically localize EGFP-tagged constructs to CBs. CstF77, a protein containing 10 HAT repeats, was not concentrated in CBs (unpublished data), indicating that the SART3/p110 HAT domain, and not all HAT domains in general, can target proteins to CBs. Although all constructs containing the HAT domain were specifically targeted to CBs, mutants lacking the COOH-terminal region

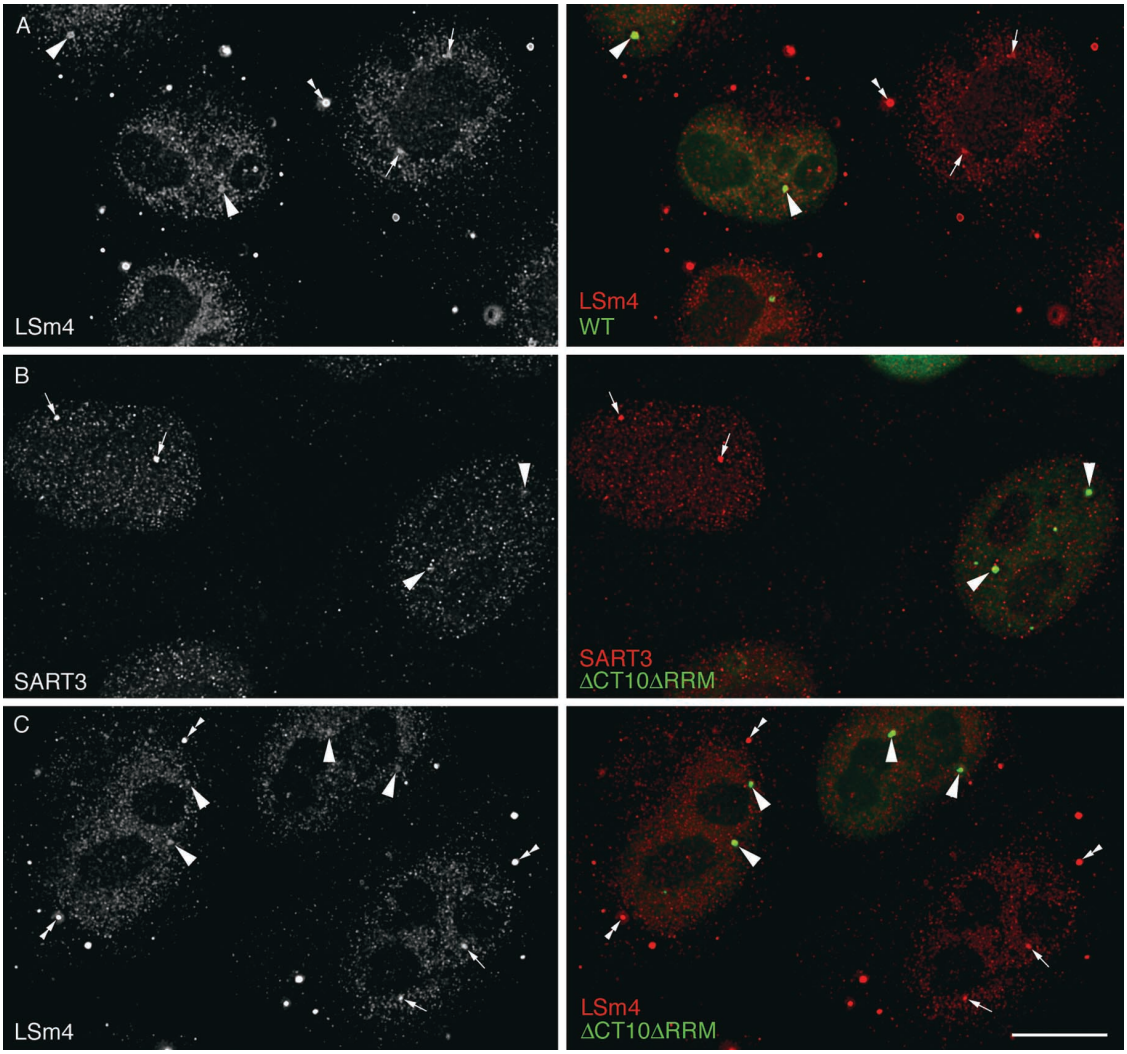

Figure 8. **Expression of ΔCT10ΔRRM–EGFP mutant reduces the concentration of endogenous SART3/p110 and LSm4 in CBs.** HeLa cells were transiently transfected with (A) WT–EGFP or (B and C) ΔCT10ΔRRM–EGFP constructs and, after fixation, immunostained with (A and C) anti-LSm4 or (B) anti-SART3/p110 antibodies. Note that anti-SART3/p110 antibodies were raised against the COOH terminus of SART3/p110 and thus do not react with fusion proteins lacking the COOH-terminal part. Projections of five optical sections are shown. CBs in transfected cells are marked by arrowheads, in nontransfected cells by arrows. Examples of cytoplasmic accumulations of LSm4 are marked by double arrowheads. Bar, 10 μm.

(ΔCT10, ΔCT10ΔRRM, and HAT) showed less intense signal than the full-length protein. Thus, although the COOH-terminal half of SART3/p110 was not specifically localized in CBs, the RRMs and/or CT-10 domain may enhance SART3/p110 retention in CBs by promoting binding to snRNPs (Shannon and Guthrie, 1991; Rader and Guthrie, 2002).

Because SART3/p110 acts during snRNP assembly, we wanted to test the hypothesis that gems, a nuclear structure often associating with CBs, are the sites of snRNP regeneration after splicing, as previously suggested (Pellizzoni et al., 1998). In HeLa cells and primary human fibroblasts, where gems are often separated from CBs, we found that SART3/p110 was not concentrated in gems, as judged by double immunofluorescence with anti-SMN (Fig. 2). Moreover, mouse embryonic fibroblasts, which lack the CB-specific protein coilin, also contain gems separate from residual CBs (Tucker et al., 2001), and these gems lacked SART3/p110 as well (Fig. 3). Therefore, our data suggest that steps in U4/U6 snRNP assembly or regeneration involving SART3/p110 are unlikely to occur in gems.

Correlation of SART3/p110 and snRNP accumulation in CBs

The spliceosomal snRNPs are concentrated in CBs even though CBs are not thought to be sites of pre-mRNA splicing (Matera, 1999). Because newly synthesized snRNPs transit CBs en route to the nucleoplasm (Sleeman and Lamond, 1999; Sleeman et al., 2001), and because snRNPs are depleted from CBs upon inhibition of transcription, a role for CBs in snRNP assembly and regeneration has been proposed (Carmo-Fonseca et al., 1992; Matera, 1999; Ogg and Lamond, 2002). If this is true, then assembly factors like SART3/p110 might interact with snRNPs in CBs. In this study, three independent lines of evidence demonstrate a correlation between SART3/p110 and snRNP accumulation

Table I. **Effect of SART3/p110 mutant expression on concentration of the endogenous SART3/p110 and LSm4 in CBs**

Overexpressed SART3/p110 protein	Endogenous SART3/p110		Endogenous LSm4	
	Fluorescent intensity (CB/nuc) ± SD (n)[a]	Significance[b]	Fluorescent intensity (CB/nuc) ± SD (n)[a]	Significance[b]
None	3.23 ± 0.81 (166)	NA	1.82 ± 0.51 (124)	NA
WT	NA	NA	1.58 ± 0.40 (130)	$P < 0.0011$
ΔCT10ΔRRM	1.74 ± 0.45 (105)	$P << 10^{-10}$	1.28 ± 0.27 (157)	$P << 10^{-10}$
ΔCT10	1.65 ± 0.49 (96)	$P << 10^{-10}$	1.26 ± 0.27 (105)	$P << 10^{-10}$

HeLa cells were transiently transfected with WT–, ΔCT10–, and ΔCT10ΔRRM–EGFP constructs and immunostained for SART3/p110 or LSm4. Ratios of SART3/p110 or LSm4 intensities in CBs with respect to their intensities in the nucleoplasm were determined. Data were collected from three independent (two in case of ΔCT10 mutant) experiments. A *t* test was run with respect to control cells (None). Data were collected for WT/SART3 because anti-SART3/p110 antibodies recognize the WT–EGFP protein. Cells expressing ΔCT10 or ΔCT10ΔRRM–EGFP exhibit a reduced level of SART3/p110 and LSm4 in CBs.
[a]Ratio of average fluorescent intensity/pixel in CB and the nucleoplasm (nuc); *n* = number of CBs evaluated.
[b]P values determined from *t* test comparing fluorescent intensity ratio for the experimental data set versus control ratios (show in "None" row) for endogenous SART3/p110 and LSm4.

in CBs, suggesting that SART3/p110 associates with CBs in a complex with snRNPs.

First, we show that SART3/p110 accumulation in CBs is dependent on the expression of the CB-specific protein coilin. In an embryonic fibroblast cell line established from a coilin$^{-/-}$ mouse, the CB components fibrillarin and Nopp140 remain concentrated in so-called residual CBs, which fail to recruit snRNPs (Tucker et al., 2001). We found that SART3/p110 was detectable in the nucleoplasm of these coilin$^{-/-}$ cells but, like snRNPs, was absent from residual CBs (Fig. 3). Thus, coilin is required for snRNP assembly into CBs (Bauer et al., 1994; Tucker et al., 2001) along with factors involved in their metabolism, such as SART3/p110.

Second, we show that SART3/p110 and snRNPs are depleted from CBs by nuclear run-on treatment, in which the activity of RNA polymerase II is preserved. In contrast, fibrillarin, coilin, and SMN remained associated with CBs after run-on treatment. The loss of SART3/p110 and snRNPs under these conditions suggests that SART3/p110 and snRNPs associate weakly with CBs and are not stable structural components of CBs. In light of recent efforts to characterize the proteomic environment of a variety of subnuclear structures (Mintz et al., 1999; Andersen et al., 2002; Lam et al., 2002), these results indicate that at least some important nuclear body components may be removed during purification and therefore subsequently escape detection. In this regard, it is noteworthy that a number of known nucleolar proteins were indeed absent in the proteomic analysis of isolated nucleoli (Andersen et al., 2002; Dundr and Misteli, 2002).

Third, we show that SART3/p110 and LSm4, which are normally concentrated in CBs (Figs. 1 and 5), are not specifically concentrated in CBs after α-amanitin treatment, indicating that SART3/p110 and LSm4 association with CBs is transcription/splicing dependent. These results coincide with previous findings (Carmo-Fonseca et al., 1992), which describe the depletion of snRNPs from CBs after α-amanitin treatment. However, in contrast to other snRNPs, the U6 snRNP component LSm4 and SART3/p110 were not concentrated in SFCs after RNA polymerase II inhibition. The dependence of SART3/p110 and snRNP accumulation in CBs on transcription and splicing is consistent with the hypothesis that CBs play an active role in snRNP metabolism and do not represent storage sites for snRNPs or SART3/p110.

CBs: sites of snRNP assembly?

The observations described here suggest that specific steps in snRNP biogenesis, namely the binding of SART3/p110 to its U4 and U6 snRNP substrates and possibly U4/U6 snRNA annealing itself, occur in CBs. We propose a model in

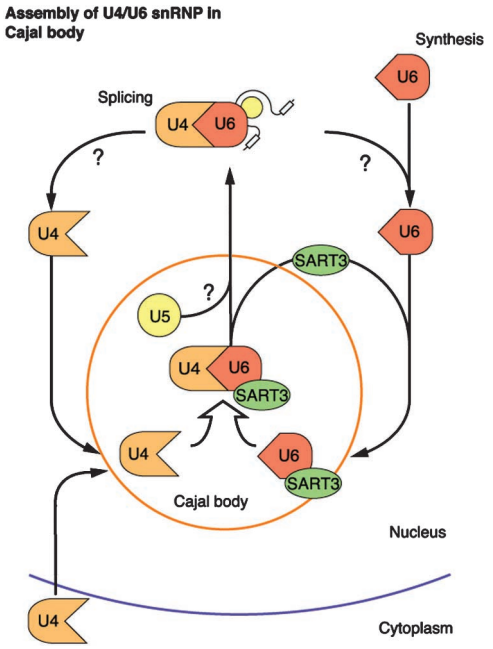

Figure 9. **A model for U4/U6 snRNP assembly in CBs.** To form a functional U4/U6 snRNP, U4 and U6 snRNAs have to be annealed. The annealing occurs after their synthesis (and reimport from the cytoplasm in the case of U4 snRNP) as well as after each round of splicing. The U4/U6 snRNP subsequently interacts with U5 snRNP (yellow ball) to form U4/U6•U5 tri-snRNP. We propose that U4/U6 snRNP assembly occurs in CBs. After splicing, the U6 snRNP is translocated to CBs as a single particle or in a complex with SART3/p110, which promotes the U4 and U6 annealing. The assembly of the U4/U6 snRNP takes place in CBs, and SART3/p110 leaves the complex as U4/U6•U5 tri-snRNP is formed. U4/U6 snRNP assembly may also occur in the nucleoplasm (not depicted), which is likely the case in cells lacking morphologically defined CBs.

which CBs are the sites of U4/U6 snRNP assembly (Fig. 9). This may occur after snRNP nuclear import and/or after each round of splicing, although direct evidence that snRNPs cycle repeatedly through CBs is currently lacking. This working hypothesis is consistent with the detection of U4 and U6 snRNAs as well as TMG cap, Sm, and LSm proteins in CBs (Carmo-Fonseca et al., 1991, 1992; Raska et al., 1991; Matera and Ward, 1993) (Fig. 5), the latter indicating that mature snRNPs are present (Matera, 1999). Importantly, newly synthesized snRNPs imported from the cytoplasm first concentrate in CBs (Sleeman and Lamond, 1999; Sleeman et al., 2001). The model is further supported by our data, which correlate snRNP and SART3/p110 association with CBs under the conditions of coilin knockout, run-on treatment, and transcription inhibition (see above). The fact that SART3/p110 associates with U6 and U4/U6 snRNPs only transiently and is not detectable in the U4/U6•U5 tri-snRNP (Bell et al., 2002; Schneider et al., 2002) is a key point in the proposal that the SART3/p110 concentration in CBs reflects its function there.

The expression of mutant SART3/p110 lacking the CT10 domain or both CT10 and RRM domains reduced the levels of endogenous SART3/p110 and LSm4 in CBs (Fig. 8; Table I). These data indicate that endogenous SART3/p110 can be depleted from CBs by overexpression of mutant proteins lacking the COOH-terminal region. These mutants also have a dominant negative effect on LSm4 localization to CBs, most likely due to the absence of the CT10 domain. This observation is in agreement with the interaction observed between the CT10 domain of Prp24, the yeast homologue of SART3/p110, and LSm proteins (Rader and Guthrie, 2002) and further support the model that SART3/p110 is in a complex with the U6 snRNP in CBs. This observation satisfies one requirement of the proposal that U4/U6 snRNP assembly occurs in CBs (Fig. 9). Moreover, these results suggest that SART3/p110 plays a role in the targeting of the U6 snRNP to CBs. In future studies, it will be important to determine how the HAT domain specifies SART3/p110 and U6 snRNP localization to CBs.

The presence of SART3/p110 in the nucleoplasm indicates that SART3/p110 binding to its substrates and/or U4/U6 annealing may also occur outside CBs. In cells lacking morphologically defined CBs, U4/U6 assembly and recycling likely takes place in the nucleoplasm, although it is currently unknown whether other CB components, such as nucleoplasmic coilin, also participate. The other possibility is that besides snRNP regeneration, nucleoplasmic SART3/p110 may be involved in other nuclear processes, as suggested by others (Harada et al., 2001; Liu et al., 2002).

Splicing involves not only unwinding of U4 and U6 snRNAs but also rearrangements within other snRNPs (Staley and Guthrie, 1998). We speculate that CBs could be involved in the assembly and/or recycling of snRNPs other than U4/U6, for example the U4atac/U6atac snRNP, the U4/U6•U5 tri-snRNP, and/or the U2 snRNP. This proposal is supported by the recent finding that a 61-kD protein involved in formation of the U4/U6•U5 and the U4atac/U6atac•U5 tri-snRNPs is also present in CBs (Makarova et al., 2002; Schneider et al., 2002). Interestingly, the U4atac/U6atac snRNP also contains LSm proteins (Schneider et al., 2002), suggesting that SART3/p110 may also promote annealing of the U4atac/U6atac snRNP. The concentration of these processes in CBs might represent an efficient pathway for the assembly and recycling of transcription and splicing factors in highly active cells with elevated levels of transcription and splicing (Boudonck et al., 1998; Gall et al., 1999; Pena et al., 2001).

Materials and methods

Cell lines and antibodies

HeLa cells, WI-38 primary fibroblasts (passages 16–18), and mouse embryonic fibroblasts 42 (coilin$^{-/-}$) and 26 (coilin$^{+/+}$) (Tucker et al., 2001) were cultured in DME supplemented with 10% fetal calf serum, penicillin, and streptomycin (GIBCO BRL). Rabbit anti-SART3/p110 antibodies were raised against the COOH-terminal 16 amino acids (PKMSNADFAKLFLRKC) and affinity purified. The following additional antibodies were used: mAb anti-coilin (5P10) (Almeida et al., 1998; provided by M. Carmo-Fonseca, Universidade de Lisboa, Lisboa, Portugal), mAb anti-SMN (2B1) (provided by G. Dreyfuss, University of Pennsylvania School of Medicine, Philadelphia, PA; Liu and Dreyfuss, 1996), mAb anti-TMG (Oncogene Research Products), mAb anti-fibrillarin (17C12) (Yang et al., 2001; provided by K. Koberna and I. Raška, Institute of Experimental Medicine, Prague, Czech Republic), mAb SC-35 (Fu and Maniatis, 1990), rat mAb anti-BrdU (Harlan Sera Lab), and a rabbit antibody against LSm4 (provided by T. Achsel and R. Luhrmann, Max Planck Institute for Biophysical Chemistry, Göttingen, Germany; Achsel et al., 1999).

SART3/p110 cloning and protein tagging

The SART3/p110 gene was amplified from 293 cell RNA by RT-PCR in two pieces, using DNA oligonucleotides A (GAATTCGCCACCATGGCGACTGCGGCCGAAACCTCGGC) and B (GCTATCCCAGAGTTCCCGGGCTTTCTGC) for the 5′ portion (nt 1–1474) and C (GCAGAAAGCCCGGGAACTCTGGGATAGC) and D (GGAGATCTGACTTTCTCAGAAACAGCTTGGCAAAATCGGCATTGG) for the 3′ portion (nt 1466–2889). Oligonucleotide A contained an EcoRI restriction site as well as a Kozak sequence, oligos B and C contained an XmaI site, and D contained a BglII site. Reverse transcription was performed using MMLV reverse transcriptase (GIBCO BRL), and PCR was performed using Pfu polymerase (Stratagene) according to the manufacturer's instructions. The two fragments were sequentially ligated into the BglII, XmaI, and EcoRI sites of plasmid pTYB4 (New England Biolabs, Inc.), and the entire EcoRI–BglII fragment was subcloned into the EcoRI–BamHI sites of pBOS-H2BGFP (BD Biosciences). Three independent bacterial transformants were sequenced (at the University of California San Francisco Biological Resource Center), revealing two silent mutations (A127G and C2815T) as well as a G507C mutation that results in a Gly→Ala change relative to the sequence in GenBank/EMBL/DDBJ (accession no. D63879). Full-length SART3/p110 as well as deletion mutants (ΔCT10 aa 1–950; ΔCT10ΔRRM aa 1–702, ΔHAT aa 581–963, and HAT aa 119–702) were amplified by Expand long template PCR system (Roche) and cloned into EGFP-N1 and -C3 vectors (CLONTECH Laboratories, Inc.) using BglII and EcoRI sites. The N-TERM (aa 1–127) fusion construct was cloned using HindIII and KpnI sites into EGFP-N2 vector (CLONTECH Laboratories, Inc.) containing at the COOH terminus three tandem repeats of the NLS from simian virus large T-antigen (gift of W. Haubensak, Max Planck Institute of Molecular Cell Biology and Genetics). The NLS signal was cloned from EYFP-Nuc vector (CLONTECH Laboratories, Inc.) using BsrGI and AflII sites.

The mouse LSm8 cDNA was obtained from R. Luhrmann and T. Achsel. The mouse LSm8 protein has the same amino acid sequence as its human homologue (Achsel et al., 1999). The full-length cDNA was amplified by Expand long template PCR and cloned into EYFP-N1 vector using BglII and KpnI restriction sites.

All fusion constructs were confirmed by sequencing. Fugene 6 (Roche) was used for transfection of cells with the SART3/p110–EGFP and LSm8–EYFP constructs.

Indirect immunofluorescence

Cells were fixed in 4% paraformaldehyde (Sigma-Aldrich) for 10 min, permeabilized for 5 min with 0.2% Triton X-100 (Sigma-Aldrich), and incubated with the indicated antibodies. Secondary anti–mouse antibodies conjugated with TRITC or FITC, anti–rat antibody conjugated with FITC,

and anti–rabbit antibodies conjugated with TRITC, FITC, or Cy5 (Jackson ImmunoResearch Laboratories) were used. Immunodetection of SART3/p110 or LSm4 in cells expressing EGFP constructs was done 24–48 h after transfection. Images were collected using the DeltaVision microscope system (Applied Precision) coupled with Olympus IX70 microscope. Stacks of 25 z-sections with 200-nm z-step were collected per sample and subjected to mathematical deconvolution (SoftWorx; Applied Precision). If not indicated otherwise, the images shown here are single sections of the resulting three-dimensional reconstructions.

Run-on transcription assay

Cells were permeabilized and RNA was labeled by BrUTP as previously described (Wansink et al., 1993; Neugebauer and Roth, 1997). In brief, cells were incubated in glycerol buffer (20 mM Tris-Cl, pH 7.4, 5 mM $MgCl_2$, 25% glycerol, 0.5% PMSF, 0.5% EGTA) for 2 min at 37°C, overlaid with BTB buffer (100 mM KCl, 50 mM Tris-Cl, pH 7.4, 5 mM $MgCl_2$, 0.5 mM EGTA, 25% glycerol, 2.5% PVA, and 0.1% Triton X-100) containing 0.5 mM ATP, GTP, and CTP and 0.2 mM BrUTP, incubated for 10 min at 37°C, fixed with 4% paraformaldehyde, and processed for immunofluorescence.

Transcription inhibition

α-Amanitin treatment was performed as previously described (Carmo-Fonseca et al., 1992). HeLa cells were placed in fresh medium, and α-amanitin (Sigma) was added to a final concentration of 50 μg/ml. Cells were incubated for 5 h and prepared for immunofluorescence as described above. To test cell viability after α-amanitin treatment, the dye FM 4–64 (Molecular Probes) was added to culture medium (final concentration 16 nM). The dye incorporation into living cells was observed after 10 min and compared with untreated control cells.

Measurement of fluorescence intensities

Fluorescence intensities were quantified with MetaVue software (Universal Imaging Corp.) using deconvolved images (see above). The optical sections were merged, and the intensities in random regions of the nucleoplasm divided by the region area were taken as the values to which the intensities within the CBs were compared. CB area was defined by SART3/p110–EGFP constructs or by coilin labeling; intensities of SART3/p110 or LSm4 were measured within the CB and divided by the CB area. Data were collected from 20–50 normal-looking CBs (Fig. 6) after α-amanitin treatment and CBs in control cells, and 100–160 CBs in cells expressing different SART3/p110–EGFP mutants or control untransfected cells (Table I).

The authors are grateful to C. Guthrie for support and helpful discussions, A.G. Matera (Case Western Reserve University, Cleveland, OH) for mouse embryonic fibroblasts 42 (coilin$^{-/-}$) and 26 (coilin$^{+/+}$), M. Carmo-Fonseca for the gift of anti-coilin antibody, G. Dreyfuss for the anti-SMN antibody, K. Koberna and I. Raska for the anti-fibrillarin antibody, and T. Achsel and R. Luhrmann for the polyclonal antibody specific for LSm4 and for the LSm8 cDNA. We thank A. Bindereif for communicating unpublished results and T. Misteli, K. Kotovic, J. Geiger, and J. Görnemann for discussion and comments on the manuscript.

This work was supported by a Research Project grant (RPG-00-110-01-MGO) from the American Cancer Society, the Max Planck Gesellschaft, and National Institutes of Health grant GM21119. S.D. Rader was supported by a National Institutes of Health postdoctoral fellowship (grant 5 F32 GM18312) and by an American Heart Association postdoctoral fellowship.

Submitted: 15 October 2002
Revised: 13 January 2003
Accepted: 13 January 2003

Note added in proof. The cytoplasmic distribution of LSm proteins 1–7 and their colocalization with mRNA-degrading enzymes has been recently published (Ingelfinger, D., D.J. Arndt-Jovin, R. Lührmann, and T. Achsel. 2002. *RNA.* 8:1489–1501).

References

Achsel, T., H. Brahms, B. Kastner, A. Bachi, M. Wilm, and R. Luhrmann. 1999. A doughnut-shaped heteromer of human Sm-like proteins binds to the 3′-end of U6 snRNA, thereby facilitating U4/U6 duplex formation in vitro. *EMBO J.* 18:5789–5802.

Almeida, F., R. Saffrich, W. Ansorge, and M. Carmo-Fonseca. 1998. Microinjection of anti-coilin antibodies affects the structure of coiled bodies. *J. Cell Biol.* 142:899–912.

Andersen, J.S., C.E. Lyon, A.H. Fox, A.K. Leung, Y.W. Lam, H. Steen, M. Mann, and A.I. Lamond. 2002. Directed proteomic analysis of the human nucleolus. *Curr. Biol.* 12:1–11.

Andrade, L.E., E.K. Chan, I. Raska, C.L. Peebles, G. Roos, and E.M. Tan. 1991. Human autoantibody to a novel protein of the nuclear coiled body: immunological characterization and cDNA cloning of p80-coilin. *J. Exp. Med.* 173:1407–1419.

Bauer, D.W., C. Murphy, Z. Wu, C.H. Wu, and J.G. Gall. 1994. In vitro assembly of coiled bodies in *Xenopus* egg extract. *Mol. Biol. Cell.* 5:633–644.

Bell, M., S. Schreiner, A. Damianov, R. Reddy, and A. Bindereif. 2002. p110, a novel human U6 snRNP protein and U4/U6 snRNP recycling factor. *EMBO J.* 21:2724–2735.

Blencowe, B.J., M. Carmo-Fonseca, S.E. Behrens, R. Luhrmann, and A.I. Lamond. 1993. Interaction of the human autoantigen p150 with splicing snRNPs. *J. Cell Sci.* 105:685–697.

Boudonck, K., L. Dolan, and P.J. Shaw. 1998. Coiled body numbers in the *Arabidopsis* root epidermis are regulated by cell type, developmental stage and cell cycle parameters. *J. Cell Sci.* 111:3687–3694.

Bouveret, E., G. Rigaut, A. Shevchenko, M. Wilm, and B. Seraphin. 2000. An Sm-like protein complex that participates in mRNA degradation. *EMBO J.* 19: 1661–1671.

Carmo-Fonseca, M. 2002. New clues to the function of the Cajal body. *EMBO Rep.* 3:726–727.

Carmo-Fonseca, M., R. Pepperkok, B.S. Sproat, W. Ansorge, M.S. Swanson, and A.I. Lamond. 1991. In vivo detection of snRNP-rich organelles in the nuclei of mammalian cells. *EMBO J.* 10:1863–1873.

Carmo-Fonseca, M., R. Pepperkok, M.T. Carvalho, and A.I. Lamond. 1992. Transcription-dependent colocalization of the U1, U2, U4/U6, and U5 snRNPs in coiled bodies. *J. Cell Biol.* 117:1–14.

Carvalho, T., F. Almeida, A. Calapez, M. Lafarga, M.T. Berciano, and M. Carmo-Fonseca. 1999. The spinal muscular atrophy disease gene product, SMN: a link between snRNP biogenesis and the Cajal (coiled) body. *J. Cell Biol.* 147:715–728.

Darzacq, X., B.E. Jady, C. Verheggen, A.M. Kiss, E. Bertrand, and T. Kiss. 2002. Cajal body-specific small nuclear RNAs: a novel class of 2′-O-methylation and pseudouridylation guide RNAs. *EMBO J.* 21:2746–2756.

Dundr, M., and T. Misteli. 2002. Nucleolomics: an inventory of the nucleolus. *Mol. Cell.* 9:5–7.

Fischer, U., Q. Liu, and G. Dreyfuss. 1997. The SMN-SIP1 complex has an essential role in spliceosomal snRNP biogenesis. *Cell.* 90:1023–1029.

Frey, M.R., A.D. Bailey, A.M. Weiner, and A.G. Matera. 1999. Association of snRNA genes with coiled bodies is mediated by nascent snRNA transcripts. *Curr. Biol.* 9:126–135.

Fromont-Racine, M., A.E. Mayes, A. Brunet-Simon, J.C. Rain, A. Colley, I. Dix, L. Decourty, N. Joly, F. Ricard, J.D. Beggs, and P. Legrain. 2000. Genome-wide protein interaction screens reveal functional networks involving Sm-like proteins. *Yeast.* 17:95–110.

Fu, X.D., and T. Maniatis. 1990. Factor required for mammalian spliceosome assembly is localized to discrete regions in the nucleus. *Nature.* 343:437–441.

Gall, J.G. 2000. Cajal bodies: the first 100 years. *Annu. Rev. Cell Dev. Biol.* 16: 273–300.

Gall, J.G., M. Bellini, Z. Wu, and C. Murphy. 1999. Assembly of the nuclear transcription and processing machinery: Cajal bodies (coiled bodies) and transcriptosomes. *Mol. Biol. Cell.* 10:4385–4402.

Ganot, P., B.E. Jady, M.L. Bortolin, X. Darzacq, and T. Kiss. 1999. Nucleolar factors direct the 2′-O-ribose methylation and pseudouridylation of U6 spliceosomal RNA. *Mol. Cell. Biol.* 19:6906–6917.

Gottschalk, A., G. Neubauer, J. Banroques, M. Mann, R. Luhrmann, and P. Fabrizio. 1999. Identification by mass spectrometry and functional analysis of novel proteins of the yeast [U4/U6.U5] tri-snRNP. *EMBO J.* 18:4535–4548.

Gu, J., S. Shimba, N. Nomura, and R. Reddy. 1998. Isolation and characterization of a new 110 kDa human nuclear RNA- binding protein (p110nrb). *Biochim. Biophys. Acta.* 1399:1–9.

Haaf, T., and D.C. Ward. 1996. Inhibition of RNA polymerase II transcription causes chromatin decondensation, loss of nucleolar structure, and dispersion of chromosomal domains. *Exp. Cell Res.* 224:163–173.

Hamm, J., E. Darzynkiewicz, S.M. Tahara, and I.W. Mattaj. 1990. The trimethylguanosine cap structure of U1 snRNA is a component of a bipartite nuclear targeting signal. *Cell.* 62:569–577.

Harada, K., A. Yamada, D. Yang, K. Itoh, and S. Shichijo. 2001. Binding of a SART3 tumor-rejection antigen to a pre-mRNA splicing factor RNPS1: a

possible regulation of splicing by a complex formation. *Int. J. Cancer.* 93: 623–628.

Kiss, A.M., B.E. Jady, X. Darzacq, C. Verheggen, E. Bertrand, and T. Kiss. 2002. A Cajal body-specific pseudouridylation guide RNA is composed of two box H/ACA snoRNA-like domains. *Nucleic Acids Res.* 30:4643–4649.

Kiss, T. 2002. Small nucleolar RNAs: an abundant group of noncoding RNAs with diverse cellular functions. *Cell.* 109:145–148.

Lam, Y.W., C.E. Lyon, and A.I. Lamond. 2002. Large-scale isolation of cajal bodies from HeLa cells. *Mol. Biol. Cell.* 13:2461–2473.

Lange, T.S., and S.A. Gerbi. 2000. Transient nucleolar localization Of U6 small nuclear RNA in *Xenopus laevis* oocytes. *Mol. Biol. Cell.* 11:2419–2428.

Liu, Q., and G. Dreyfuss. 1996. A novel nuclear structure containing the survival of motor neurons protein. *EMBO J.* 15:3555–3565.

Liu, Y., J. Li, B.O. Kim, B.S. Pace, and J.J. He. 2002. HIV-1 Tat protein-mediated transactivation of the HIV-1 long terminal repeat promoter is potentiated by a novel nuclear Tat-interacting protein of 110 kDa, Tip110. *J. Biol. Chem.* 277:23854–23863.

Makarova, O.V., E.M. Makarov, S. Liu, H.P. Vornlocher, and R. Luhrmann. 2002. Protein 61K, encoded by a gene (PRPF31) linked to autosomal dominant retinitis pigmentosa, is required for U4/U6*U5 tri-snRNP formation and pre-mRNA splicing. *EMBO J.* 21:1148–1157.

Massenet, S., L. Pellizzoni, S. Paushkin, I.W. Mattaj, and G. Dreyfuss. 2002. The SMN complex is associated with snRNPs throughout their cytoplasmic assembly pathway. *Mol. Cell. Biol.* 22:6533–6541.

Matera, A.G. 1999. Nuclear bodies: multifaceted subdomains of the interchromatin space. *Trends Cell Biol.* 9:302–309.

Matera, A.G., and D.C. Ward. 1993. Nucleoplasmic organization of small nuclear ribonucleoproteins in cultured human cells. *J. Cell Biol.* 121:715–727.

Mayes, A.E., L. Verdone, P. Legrain, and J.D. Beggs. 1999. Characterization of Sm-like proteins in yeast and their association with U6 snRNA. *EMBO J.* 18:4321–4331.

Mintz, P.J., S.D. Patterson, A.F. Neuwald, C.S. Spahr, and D.L. Spector. 1999. Purification and biochemical characterization of interchromatin granule clusters. *EMBO J.* 18:4308–4320.

Neugebauer, K.M. 2002. On the importance of being co-transcriptional. *J. Cell Sci.* 115:3865–3871.

Neugebauer, K.M., and M.B. Roth. 1997. Distribution of pre-mRNA splicing factors at sites of RNA polymerase II transcription. *Genes Dev.* 11:1148–1159.

Ogg, S.C., and A.I. Lamond. 2002. Cajal bodies and coilin–moving towards function. *J. Cell Biol.* 159:17–21.

Paushkin, S., A.K. Gubitz, S. Massenet, and G. Dreyfuss. 2002. The SMN complex, an assemblyosome of ribonucleoproteins. *Curr. Opin. Cell Biol.* 14: 305–312.

Pellizzoni, L., N. Kataoka, B. Charroux, and G. Dreyfuss. 1998. A novel function for SMN, the spinal muscular atrophy disease gene product, in pre-mRNA splicing. *Cell.* 95:615–624.

Pellizzoni, L., B. Charroux, J. Rappsilber, M. Mann, and G. Dreyfuss. 2001. A functional interaction between the survival motor neuron complex and RNA polymerase II. *J. Cell Biol.* 152:75–85.

Pena, E., M.T. Berciano, R. Fernandez, J.L. Ojeda, and M. Lafarga. 2001. Neuronal body size correlates with the number of nucleoli and Cajal bodies, and with the organization of the splicing machinery in rat trigeminal ganglion neurons. *J. Comp. Neurol.* 430:250–263.

Preker, P.J., and W. Keller. 1998. The HAT helix, a repetitive motif implicated in RNA processing. *Trends Biochem. Sci.* 23:15–16.

Rader, S.D., and C. Guthrie. 2002. A conserved Lsm-interaction motif in Prp24 required for efficient U4/U6 di-snRNP formation. *RNA.* 8:1378–1392.

Raghunathan, P.L., and C. Guthrie. 1998. A spliceosomal recycling factor that reanneals U4 and U6 small nuclear ribonucleoprotein particles. *Science.* 279: 857–860.

Rappsilber, J., U. Ryder, A.I. Lamond, and M. Mann. 2002. Large-scale proteomic analysis of the human spliceosome. *Genome Res.* 12:1231–1245.

Raska, I., R.L. Ochs, L.E. Andrade, E.K. Chan, R. Burlingame, C. Peebles, D. Gruol, and E.M. Tan. 1990. Association between the nucleolus and the coiled body. *J. Struct. Biol.* 104:120–127.

Raska, I., L.E. Andrade, R.L. Ochs, E.K. Chan, C.M. Chang, G. Roos, and E.M. Tan. 1991. Immunological and ultrastructural studies of the nuclear coiled body with autoimmune antibodies. *Exp. Cell Res.* 195:27–37.

Ryan, D.E., S.W. Stevens, and J. Abelson. 2002. The 5′ and 3′ domains of yeast U6 snRNA: Lsm proteins facilitate binding of Prp24 protein to the U6 telestem region. *RNA.* 8:1011–1033.

Salgado-Garrido, J., E. Bragado-Nilsson, S. Kandels-Lewis, and B. Seraphin. 1999. Sm and Sm-like proteins assemble in two related complexes of deep evolutionary origin. *EMBO J.* 18:3451–3462.

Schneider, C., C.L. Will, O.V. Makarova, E.M. Makarov, and R. Luhrmann. 2002. Human U4/U6.U5 and U4atac/U6atac.U5 tri-snRNPs exhibit similar protein compositions. *Mol. Cell. Biol.* 22:3219–3229.

Seraphin, B. 1995. Sm and Sm-like proteins belong to a large family: identification of proteins of the U6 as well as the U1, U2, U4 and U5 snRNPs. *EMBO J.* 14:2089–2098.

Shannon, K.W., and C. Guthrie. 1991. Suppressors of a U4 snRNA mutation define a novel U6 snRNP protein with RNA-binding motifs. *Genes Dev.* 5:773–785.

Sleeman, J.E., and A.I. Lamond. 1999. Newly assembled snRNPs associate with coiled bodies before speckles, suggesting a nuclear snRNP maturation pathway. *Curr. Biol.* 9:1065–1074.

Sleeman, J.E., P. Ajuh, and A.I. Lamond. 2001. snRNP protein expression enhances the formation of Cajal bodies containing p80-coilin and SMN. *J. Cell Sci.* 114:4407–4419.

Staley, J.P., and C. Guthrie. 1998. Mechanical devices of the spliceosome: motors, clocks, springs, and things. *Cell.* 92:315–326.

Tharun, S., W. He, A.E. Mayes, P. Lennertz, J.D. Beggs, and R. Parker. 2000. Yeast Sm-like proteins function in mRNA decapping and decay. *Nature.* 404:515–518.

Tomasevic, N., and B.A. Peculis. 2002. *Xenopus* LSm proteins bind U8 snoRNA via an internal evolutionarily conserved octamer sequence. *Mol. Cell. Biol.* 22:4101–4112.

Tucker, K.E., M.T. Berciano, E.Y. Jacobs, D.F. LePage, K.B. Shpargel, J.J. Rossire, E.K. Chan, M. Lafarga, R.A. Conlon, and A.G. Matera. 2001. Residual Cajal bodies in coilin knockout mice fail to recruit Sm snRNPs and SMN, the spinal muscular atrophy gene product. *J. Cell Biol.* 154:293–307.

Tuma, R.S., J.A. Stolk, and M.B. Roth. 1993. Identification and characterization of a sphere organelle protein. *J. Cell Biol.* 122:767–773.

Tycowski, K.T., Z.H. You, P.J. Graham, and J.A. Steitz. 1998. Modification of U6 spliceosomal RNA is guided by other small RNAs. *Mol. Cell.* 2:629–638.

Vidal, V.P., L. Verdone, A.E. Mayes, and J.D. Beggs. 1999. Characterization of U6 snRNA-protein interactions. *RNA.* 5:1470–1481.

Wansink, D.G., W. Schul, I. van der Kraan, B. van Steensel, R. van Driel, and L. de Jong. 1993. Fluorescent labeling of nascent RNA reveals transcription by RNA polymerase II in domains scattered throughout the nucleus. *J. Cell Biol.* 122:283–293.

Will, C.L., and R. Luhrmann. 2001. Spliceosomal UsnRNP biogenesis, structure and function. *Curr. Opin. Cell Biol.* 13:290–301.

Yang, J.M., S.J. Baserga, S.J. Turley, and K.M. Pollard. 2001. Fibrillarin and other snoRNP proteins are targets of autoantibodies in xenobiotic-induced autoimmunity. *Clin. Immunol.* 101:38–50.

Young, P.J., T.T. Le, N. thi Man, A.H. Burghes, and G.E. Morris. 2000. The relationship between SMN, the spinal muscular atrophy protein, and nuclear coiled bodies in differentiated tissues and cultured cells. *Exp. Cell Res.* 256: 365–374.

Zhou, Z., L.J. Licklider, S.P. Gygi, and R. Reed. 2002. Comprehensive proteomic analysis of the human spliceosome. *Nature.* 419:182–185.